

Compositional effect on the dielectric properties of high- k titanium silicate thin films deposited by means of a cosputtering process

Cite as: J. Vac. Sci. Technol. A **24**, 600 (2006); <https://doi.org/10.1116/1.2180267>

Submitted: 19 August 2005 • Accepted: 31 January 2006 • Published Online: 04 May 2006

D. Brassard, D. K. Sarkar, M. A. El Khakani, et al.



View Online



Export Citation

ARTICLES YOU MAY BE INTERESTED IN

High- k titanium silicate thin films grown by reactive magnetron sputtering for complementary metal-oxide-semiconductor applications

Journal of Vacuum Science & Technology A **22**, 851 (2004); <https://doi.org/10.1116/1.1722530>

Substrate biasing effect on the electrical properties of magnetron-sputtered high- k titanium silicate thin films

Journal of Applied Physics **102**, 034106 (2007); <https://doi.org/10.1063/1.2759196>

High- k titanium silicate dielectric thin films grown by pulsed-laser deposition

Applied Physics Letters **80**, 294 (2002); <https://doi.org/10.1063/1.1435072>



Advance your science and
career as a member of

AVS

LEARN MORE



Compositional effect on the dielectric properties of high-*k* titanium silicate thin films deposited by means of a cosputtering process

D. Brassard, D. K. Sarkar, and M. A. El Khakani^{a)}

Institut National de la Recherche Scientifique INRS-Énergie, Matériaux et Télécommunications, 1650, Boulevard Lionel-Boulet, C.P. 1020, Varennes, Québec J3X 1S2, Canada

L. Ouellet

DALSA Semiconductor, 18, Boulevard de l'Aéroport, Bromont, Québec J2L 1S7, Canada

(Received 19 August 2005; accepted 31 January 2006; published 4 May 2006)

We report on the successful growth of high dielectric constant (high-*k*) titanium silicate $\text{Ti}_x\text{Si}_{1-x}\text{O}_2$ thin films of various compositions ($0 \leq x \leq 1$) at room temperature from the cosputtering of SiO_2 and TiO_2 targets. The developed process is shown to offer the latitude required to achieve not only a precise control of the film composition but an excellent morphology (i.e., dense films with low roughness) as well. The Fourier transform infrared and x-ray photoelectron spectroscopy characterizations have evidenced the presence of Ti–O–Si type of atomic environments, which is the fingerprint of the titanium silicate phase. The titanium silicate films are found to exhibit excellent dielectric properties with very low dielectric losses [$\tan(\delta) < 0.02$] regardless of their composition. The dielectric constant of the films is found to increase with their TiO_2 content from 4 (for pure SiO_2 films) to 45 (for TiO_2). On the other hand, increasing the TiO_2 content of the films is also shown to degrade significantly their leakage current. Nevertheless, titanium silicate films with almost equiatomic composition ($x \sim 0.45$) are found to exhibit an excellent trade-off between a high-*k* value (~ 18) and low leakage current ($\sim 5 \times 10^{-7}$ A/cm² at 1 MV/cm). Finally, the compositional dependence of the dielectric properties of the $\text{Ti}_x\text{Si}_{1-x}\text{O}_2$ films is discussed in terms of bonding states and optical band gap. © 2006 American Vacuum Society. [DOI: 10.1116/1.2180267]

I. INTRODUCTION

The aggressive scaling trend of the microelectronic devices and the development of advanced analog and radio-frequency (rf) integrated circuit applications trigger a tremendous demand for the development and the integration of suitable high dielectric constant (high-*k*) materials.^{1–4} For example, the traditional SiO_2 and SiON gate dielectrics of metal-oxide-semiconductor field effect transistors (MOSFETs) are now reaching a thickness regime (~ 1 nm) where fundamental issues such as high tunneling leakage current and boron diffusion appear.^{1,2} Thus, high-*k* materials emerge as a mean to reach the high capacitance density required for the transistors operation with physically thicker gate dielectrics. On the other hand, advanced analog and rf circuit applications create a pressing need for the development of integrated metal-insulator-metal (MIM) capacitors with higher capacitance density, low leakage current, and good voltage linearity.^{3,4} High-*k* materials are thus seen as an alternative way to reach the aggressive electrical performances required for MIM applications.

It is a fact that, despite the important worldwide research effort over the last years, the development of high-*k* materials that fulfill the highly aggressive criteria required for their successful integration remains a challenging task.¹ Indeed, even if numerous high-*k* materials including transition metal oxides [such as TiO_2 ($k \sim 75$),⁵ ZrO_2 ($k \sim 20$),⁶ and HfO_2

($k \sim 15$ – 20) (Refs. 4 and 7)] were considered, the replacement of the traditional SiO_2 ($k = 3.9$) insulator still poses substantial problems. For example, the task of finding the appropriate high-*k* dielectric is complicated by process related limitations such as the low thermal budget required for back-end integration of MIM devices.¹ Processes must thus be developed to enable the growth of high quality dielectrics at low deposition temperatures. In addition, high-*k* dielectrics generally have a smaller band gap compared to SiO_2 and thus show higher leakage currents and lower breakdown fields.² Nevertheless, among the various high-*k* dielectrics, metal silicates (i.e., mixtures of SiO_2 with a metal oxide) have been identified as promising dielectric candidates as they offer the interesting possibility to combine the advantages from both SiO_2 (low leakage current and high breakdown field) and metal oxides (i.e., high *k*).^{2,8–13} Metal silicates also generally have a larger band gap compared to their metal oxide counterpart^{2,14} and they exhibit a better thermal stability against crystallization.^{2,13} However, materials from this group have lower dielectric constant than metal oxides and most of the silicates such as $\text{Hf}_{0.5}\text{Si}_{0.5}\text{O}_2$ and $\text{Zr}_{0.5}\text{Si}_{0.5}\text{O}_2$ are thus limited to a *k* in the 10–15 range.^{2,13,15} Titanium silicates (also referred to as $\text{TiO}_2/\text{SiO}_2$ mixed oxides) appear as a very interesting candidate as they can exhibit higher dielectric constants ($k > 20$) can be achieved for $\text{Ti}_{0.5}\text{Si}_{0.5}\text{O}_2$,^{8–11} without suffering from the weaknesses of the metal oxides. In this context, only very few works have been reported so far on the electrical properties of titanium

^{a)} Author to whom correspondence should be addressed; electronic mail: elkhakani@emt.inrs.ca

silicate thin films, and a complete understanding of the relationship between their composition, microstructure, and electrical properties is still to be established.

In this article, we report on the development of a room-temperature cosputtering process for the growth of high- k titanium silicate $\text{Ti}_x\text{Si}_{1-x}\text{O}_2$ thin films of various compositions ($0 \leq x \leq 1$). We present a systematic investigation of the effect of the composition on the morphological, microstructural, optical, and dielectric properties of the films. Our results demonstrate that by controlling the film composition, it is possible to achieve $\text{Ti}_x\text{Si}_{1-x}\text{O}_2$ films that exhibit not only a high- k value but low leakage current density as well. The composition dependence of the dielectric properties of the films is additionally shown to correlate well with the variation of their optical band gap and bonding states.

II. EXPERIMENT

The $\text{Ti}_x\text{Si}_{1-x}\text{O}_2$ films were sputter deposited from the concomitant cosputtering of a pressed-powder TiO_2 target (99.9% purity) and a fused SiO_2 target (99.95% purity) using a multicathode rf-magnetron sputtering system. The composition of the films (i.e., x , which also refers to the TiO_2 content of the films; both terms may be used indifferently throughout this article) was controlled by independently varying the power (P) applied on the 3-in.-diam targets in the 0–250 W range. The system base pressure was of about of 2×10^{-8} Torr. During deposition, high-purity Ar and O_2 gases were introduced in the chamber and their relative flow rates were monitored to keep a low operating pressure of 1.5 mTorr and a $[\text{O}_2]/([\text{O}_2] + [\text{Ar}])$ flow rate ratio of 20%.⁸ The films were simultaneously deposited on both Si (100) and Pt-coated Si substrates, and their temperature was kept at $\sim 25^\circ\text{C}$ during deposition. No postdeposition annealings were performed.

The chemical composition and bonding states of the films were systematically investigated using x-ray photoelectron spectroscopy (XPS) (ESCALAB 220I-XL spectrophotometer, equipped with an $\text{Al } K_\alpha$ monochromatic source), both before and after *in situ* surface cleaning by means of 5 keV Ar^+ ions sputtering. Fourier transform infrared (FTIR) spectroscopy absorbance measurements were performed using a BOMEM-Michelson-100 spectrometer with a bare Si wafer as reference. The thickness, density, and roughness of the films were determined from their x-ray reflectivity (XRR) spectra¹⁶ acquired by means of a Philips X'pert diffractometer using $\text{Cu } K_\alpha$ radiation. The optical properties and thicknesses of the films were characterized in the 1.0–5.5 eV range with a variable angle spectroscopic ellipsometry using the J. A. Woollam Co. ellipsometer. The optical constants of the films (index of refraction n , absorption coefficient, and optical band gap E_g) were obtained by fitting the acquired spectra with the WVASE32 software using the Cauchy-Lorentz model.^{14,17} The thickness of the films was in the 50–120 nm range. For the electrical characterizations, the titanium silicate films deposited on Pt-coated Si substrates were integrated into metal-insulator-metal (MIM) capacitors with Al contacts as top electrodes. The dielectric constant and dissipa-

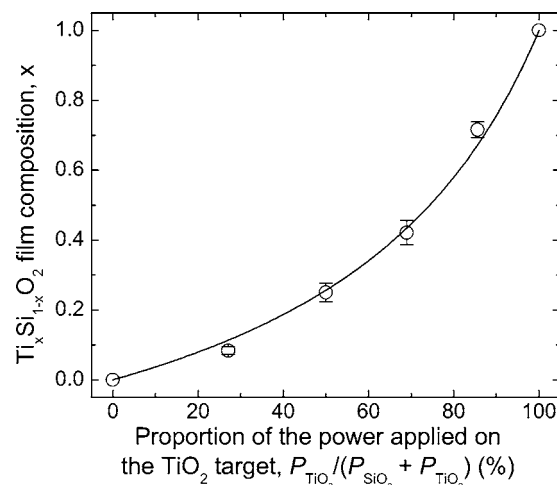


FIG. 1. Variation of the TiO_2 content of the cosputtered deposited $\text{Ti}_x\text{Si}_{1-x}\text{O}_2$ films as a function of the power applied on the TiO_2 and the SiO_2 targets.

tion factor $\tan(\delta)$ of the films were obtained from the complex impedance characterization (acquired from an HP4192a) of the MIM devices. An HP4145A picoammeter was used to collect the current-voltage (I - V) characteristics.

III. RESULTS AND DISCUSSION

Figure 1 shows the effect of the relative power applied on the TiO_2 target on the $\text{Ti}_x\text{Si}_{1-x}\text{O}_2$ film composition (as determined by XPS). As one would expect, the TiO_2 content of the films is seen to increase systematically as the power applied on the TiO_2 target is increased. The composition of the titanium silicate films can thus be precisely controlled over the entire composition range (i.e., $0 \leq x \leq 1$) with the cosputtering technique. The solid line shown in Fig. 1 represents a model that considers that the deposition rate of each target is directly proportional to the power applied to it.¹⁸ The best fit to our experimental data (Fig. 1) indicates that, for a given power value, the deposition rate (in molecules/s) from the SiO_2 target is ~ 3 times larger than that from the TiO_2 target. This relatively large difference in deposition rate (which is due to a difference in sputtering yields) is likely due to differences in both chemical bondings and atomic mass ratios involved in the sputtering process. In addition, the different densification levels of the targets (i.e., dense fused silica versus pressed TiO_2 powder pellets) may also contribute to the observed difference in the deposition rates of SiO_2 and TiO_2 films. These results show that by independently controlling the rf power applied to each of the SiO_2 and TiO_2 targets, one can precisely adjust the film composition (x) of the resulting $\text{Ti}_x\text{Si}_{1-x}\text{O}_2$ silicate thin films.

Figure 2(a) shows the O 1s, Si 2p, and Ti 2p core level XPS spectra of the $\text{Ti}_x\text{Si}_{1-x}\text{O}_2$ films with various compositions ($0 \leq x \leq 1$). The O 1s and Si 2p binding energies are found to appear, respectively, at 533.0 and 103.4 eV for the SiO_2 sputtered films, while the O 1s and Ti 2p_{3/2} peak positions are located at 530.2 and 458.7 eV, respectively, for the TiO_2 sputtered films. These binding energies correspond to the value typically quoted for SiO_2 and TiO_2 .^{19,20} As the

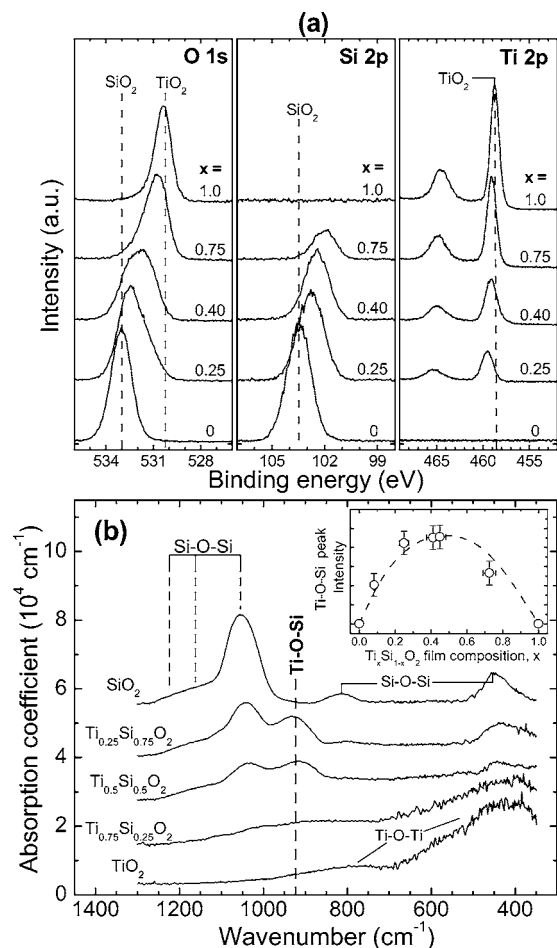


FIG. 2. Effect of the composition x of the cosputtered $\text{Ti}_x\text{Si}_{1-x}\text{O}_2$ thin films on (a) the high-resolution XPS spectra of the O 1s, Si 2p, and Ti 2p core levels and on (b) the 350–1300 cm^{-1} region of the FTIR absorbance spectra. The inset shows the variation of the Ti–O–Si peak intensity with the composition of the films.

TiO_2 content of the films is increased, the positions of the O 1s, Si 2p, and Ti 2p core level peaks are clearly seen to shift continuously towards lower binding energies, in accordance with peak position reported for silicate films.^{19,21} These shifts show that the charge on the O and Si atoms is affected by the introduction of Ti atoms in their neighborhood and conversely that Ti atoms are affected by the presence of nearby Si in the silicate films. In addition, one can note that the O 1s spectra appear as a single peak for all the film compositions (as opposed to the appearance of two distinct peaks that could reflect the presence of segregated SiO_2 and TiO_2 phases). The latter observations indicate that the sputtered material from both the SiO_2 and the TiO_2 targets was mixed at the atomic level during the deposition process to form the silicate phase rather than a mixture of separate phases of SiO_2 and TiO_2 . The O 1s peak is also seen to show significantly larger full width at half maximum (FWHM) for the silicate films having an intermediate composition (2.4 eV for $\text{Ti}_{0.4}\text{Si}_{0.6}\text{O}_2$ compared to 1.49 and 1.23 eV for SiO_2 and TiO_2 , respectively), thus confirming the concomitant presence of different environments (such as of Ti–O–Ti, Si–O–

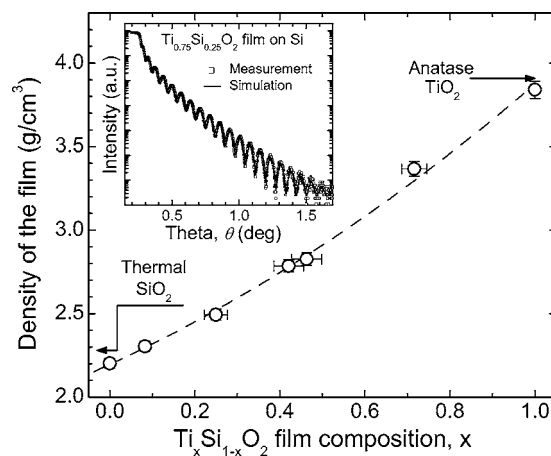


FIG. 3. Density of the cosputtered $\text{Ti}_x\text{Si}_{1-x}\text{O}_2$ thin films, as determined from XRR measurements, as a function of their composition. Literature density values for thermal SiO_2 (Ref. 24) and anatase TiO_2 are also shown on the graph. The inset shows a typical XRR curve for a cosputtered $\text{Ti}_{0.75}\text{Si}_{0.25}\text{O}_2$ film deposited on Si with its corresponding simulated spectrum.

Si, and Si–O–Ti) around the oxygen atoms in the silicate films. Finally regardless of the film composition ($0 \leq x \leq 1$), no metallic bondings (such as Ti–Si, Si–Si, or Ti–Ti) were detected in the spectra. Moreover, the $[\text{O}]/([\text{Si}]+[\text{Ti}])$ oxygen ratio of the films was of about 2.0, thus providing evidence of the formation of completely oxidized films.

The FTIR characterization of the silicate films has permitted to gain more insights on their bonding states. Figure 2(b) reveals the presence of an absorption band at 920–950 cm^{-1} which is due to the presence of Ti–O–Si bondings^{20,22} (that is the fingerprint of the titanium silicate phase). In addition, several other absorption bands are seen in the spectra, indicating thereby the presence of some Si–O–Si environments (for which peaks are observed at 1100, 1060, 800, and 450 cm^{-1})²² in the silicate films. In addition, the broad absorption peak (between 400 and ~ 800 cm^{-1}) observed for the TiO_2 -rich films is characteristic of Ti–O–Ti type of bonding in amorphous TiO_2 .²³ By deconvoluting the various above-cited absorption bands (as previously detailed in Refs. 11 and 12), we were able to extract the intensity of the Ti–O–Si band as a function of the film composition, as shown in the inset of Fig. 2(b). Indeed, it is seen that the Ti–O–Si band intensity versus film composition curve presents a parabolic-like dependence with a maximum located around intermediate x values ($x \sim 0.5$). Such a behavior is indicative of a random mixture of Ti, Si, and O atoms in the silicates films, as it has been discussed in Ref. 22.

Figure 3 shows the variation of the density of the $\text{Ti}_x\text{Si}_{1-x}\text{O}_2$ films as a function of their composition, as determined from XRR measurements. The density of the films is found to increase systematically as their TiO_2 content is increased, with a very slight deviation from linearity. Interestingly, the measured densities for both sputtered SiO_2 and TiO_2 films (i.e., 2.20 and 3.84 g/cm^3 , respectively) are very comparable with values typically quoted for thermal SiO_2 and anatase TiO_2 [2.28 g/cm^3 (Ref. 24) and 3.91 g/cm^3 , respectively]. The density of titanium silicate films at interme-

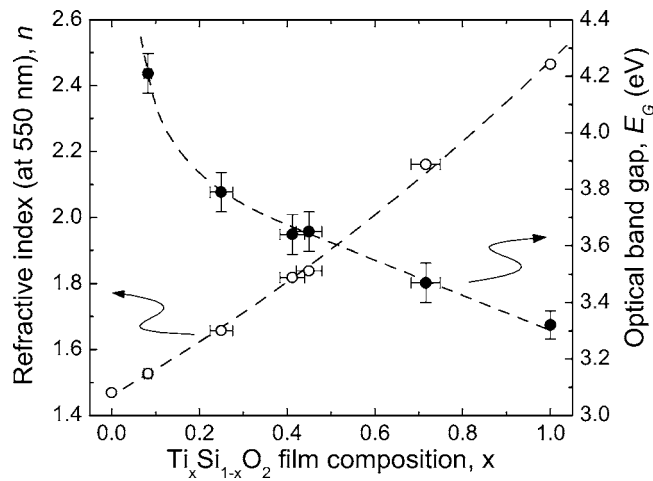


FIG. 4. Refractive index (at 550 nm wavelength) and optical band gap variations with the composition of the cosputtered $\text{Ti}_x\text{Si}_{1-x}\text{O}_2$ thin films.

diate compositions ($x \sim 0.45$) is found to be of 2.85 g/cm^3 . On the other hand, the roughness of the silicate films, derived from the analysis of the XRR measurements,¹⁶ is found to be very low ($\sim 1 \text{ nm}$). Thus, the XRR characterization confirms that titanium silicate thin films with excellent morphological characteristics can be grown from the developed cosputtering process.

Figure 4 shows the variation of the optical properties of the films, obtained from ellipsometry measurements, as a function of their composition. The index of refraction at 550 nm is seen to vary from 1.47 for SiO_2 to 2.47 for TiO_2 , in agreement with the literature values.²⁵ The index of refraction is found to increase almost linearly with the TiO_2 content of the films in a similar way to the film density variation (see Fig. 3). [In fact, a very good linear correlation is obtained in a cross plot of the density of the films with their refractive index (not shown here).] Similar variations of the refractive index with composition have been reported for TiO_2 - SiO_2 composite films.^{22,25} In contrast, the optical band gap of the titanium silicate films shows a rather different variation with the composition (Fig. 4). Indeed, for the SiO_2 films, no absorption was observed in the measured energy range, thus indicating that their band gap is larger than 5.5 eV (in accordance with the reference value of 9.0 eV for SiO_2).² On the other hand, as soon as some TiO_2 is incorporated in the films, their optical band gap is found to decrease very rapidly to a value of 4.2 eV. As the TiO_2 content of the $\text{Ti}_x\text{Si}_{1-x}\text{O}_2$ films is further increased, their band gap continues to decrease to reach a value of ~ 3.65 for $x \sim 0.45$. For higher TiO_2 content, the band gap continues to diminish but at a more slower rate to reach a value of ~ 3.3 eV for the TiO_2 films, in agreement with the values reported in the literature.^{2,20} Somewhat similar variations of the band gap with composition were also reported for phase separated $\text{TiO}_2/\text{SiO}_2$ thin films.^{20,26} In these latter cases, the increase of the band gap compared to TiO_2 was generally interpreted by considering a quantum-size effect caused by the variation of the size of the segregated TiO_2 nanoparticles in the

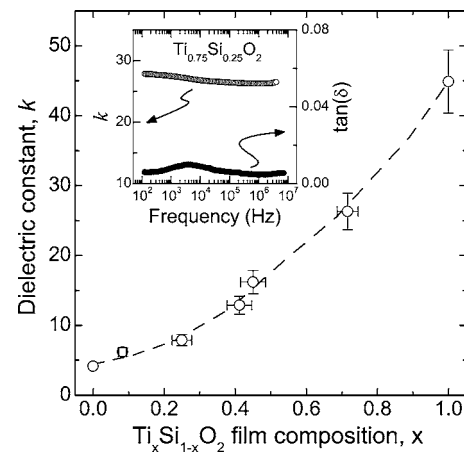


FIG. 5. Dielectric constant of the cosputtered $\text{Ti}_x\text{Si}_{1-x}\text{O}_2$ thin films as a function of their composition. The inset shows typical dielectric constant and dissipation factor vs frequency curves (in the case of $\text{Ti}_{0.75}\text{Si}_{0.25}\text{O}_2$ film).

films.^{20,26} However, as our cosputtered titanium silicate films appear to consist of a random mixture of Ti, Si, and O atoms with no evidence of the presence of any segregated TiO_2 phase (see Fig. 2 and associated discussion), our results rather suggest that the introduction of Ti atoms in the SiO_2 network creates states within the SiO_2 band gap and thus absorption at much lower photon energies.

The effect of the composition on the dielectric constant k (measured at 1 MHz) of the titanium silicate films is shown in Fig. 5. The dielectric properties of the films were measured in the 100 Hz–10 MHz frequency range (a typical measurement is shown in the inset of Fig. 5). Regardless of the film composition ($0 \leq x \leq 1$), the $\text{Ti}_x\text{Si}_{1-x}\text{O}_2$ films were found to exhibit very low dispersion of the dielectric constant together with very low dissipation factors [$\tan(\delta) < 0.02$] over the entire frequency range investigated (as illustrated in the inset of Fig. 5). This demonstrates that the cosputtered titanium silicate films possess excellent dielectric properties over all the composition range. In addition, their dielectric constant is found to increase systematically as their TiO_2 proportion is increased. Indeed, k value increases from ~ 7 for the titanium silicate films containing $\sim 10 \text{ at. \% TiO}_2$ to ~ 28 for films containing $\sim 75 \text{ at. \% TiO}_2$. The equiatomic $\text{Ti}_{0.5}\text{Si}_{0.5}\text{O}_2$ films exhibit a k value of ~ 18 . This value is found to be very comparable to theoretical predictions for titanium silicate.²⁷ On the other hand, higher k values (~ 20 – 35) were reported in the literature for $\text{Ti}_{0.5}\text{Si}_{0.5}\text{O}_2$ films.^{8–11} This small difference is thought to be due to the rather low deposition temperature ($\sim 25^\circ\text{C}$) used in the present cosputtering process (in comparison with typical postdeposition annealing and deposition temperatures in the 300 – 800°C range.^{8–11} Such a low deposition temperature is expected to lead to a more disordered amorphous microstructure which, in turn, might lower the dielectric constant of the films in comparison with their more ordered or ultimately crystalline counterparts.⁹ Nevertheless, it is worth noting that a k value of ~ 18 for $\text{Ti}_{0.5}\text{Si}_{0.5}\text{O}_2$ is definitely higher than the values obtained for other silicate films (e.g., k is in the 9–14

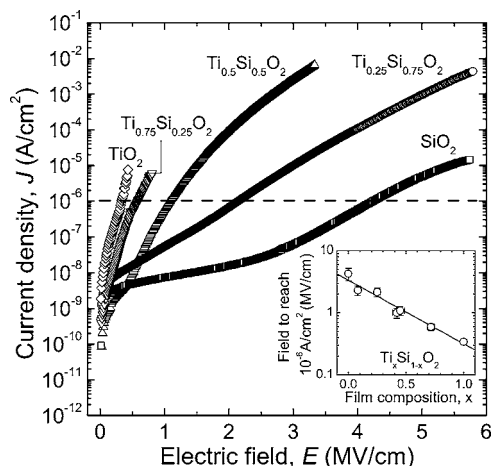


FIG. 6. Leakage current density vs electric field curves for cosputtered $\text{Ti}_x\text{Si}_{1-x}\text{O}_2$ thin films with various compositions. The inset shows the composition dependence of the soft breakdown field of the cosputtered $\text{Ti}_x\text{Si}_{1-x}\text{O}_2$ films.

range for $\text{Hf}_{0.5}\text{Si}_{0.5}\text{O}_2$ and 12.6 for $\text{Zr}_{0.5}\text{Si}_{0.5}\text{O}_2$).^{2,10} On the other hand, one can note that the observed k versus composition relationship shows a downward bowing with a slow increase of the dielectric constant until the TiO_2 proportion reaches $\sim 40\%$, followed by a rapid increase at higher TiO_2 contents. This tendency suggests that the increased polarizability brought by the presence of Ti atoms depends strongly on their surrounding environment in the silicate films. Indeed, the very high dielectric constant shown by TiO_2 is well known to arise from large displacements of the sixfold coordinated Ti ions in the TiO_6 octahedral complex when an electric field is applied (this mechanism is referred to as soft phonons or the pseudo-Jahn-Teller-effect).² However, in the titanium silicate films with low TiO_2 concentrations, the Ti atoms are predominantly fourfold coordinated²⁰ since they are inserted into the SiO_2 tetrahedral network to create Ti–O–Si bondings (as seen in our FTIR measurements [Fig. 2(b)]). Thus, the rather small increase of the dielectric constant for the silicate films with low Ti concentrations suggests that the polarizability of the Ti ions inserted in Ti–O–Si environments is much smaller than that of the Ti atoms in an octahedral complex. On the other hand, when the TiO_2 content of the films is increased, the environment around the Ti atoms gradually evolves toward an octahedral coordination,²⁰ as seen from the predominant presence of the Ti–O–Ti broad feature in their FTIR spectra [Fig. 2(b)], thereby explaining the rapid increase of k observed at high TiO_2 contents.

Figure 6 shows the leakage current density versus electric field characteristics for the $\text{Ti}_x\text{Si}_{1-x}\text{O}_2$ based MIM capacitors as a function of the TiO_2 content of the films. In addition, the variation of the soft breakdown field (defined as the electric field required to reach a leakage current density of 10^{-6} A/cm^2 ; see the dashed line in Fig. 6) as a function of the composition of the films is shown in the inset of Fig. 6. As expected, the SiO_2 films are found to show the lowest leakage current of the group, with the highest soft break-

down field ($\sim 4.5 \text{ MV/cm}$). Nevertheless, one should note that the sputtered SiO_2 films exhibit a leakage current density higher than that of plasma-enhanced chemical-vapor deposition (PECVD)-grown and postannealed SiO_2 MIM capacitors.²⁸ This difference is thought to be due to a reduced density of active defects in the PECVD SiO_2 films, as a consequence of their subsection to a postdeposition forming gas annealing treatment at 420°C . In addition, the leakage current is clearly seen to rise markedly as the TiO_2 content of the films is increased and, conversely, their soft breakdown field is found to drop rapidly, reaching a value of $\sim 0.3 \text{ MV/cm}$ for the room-temperature sputtered TiO_2 films. This strong variation of the leakage current and breakdown field of the $\text{Ti}_x\text{Si}_{1-x}\text{O}_2$ films can be well correlated with the variation of their optical band gap (see Fig. 4). A reduction of the band gap definitely reduces the effective barrier against the injection of charges inside the dielectric and consequently leads to a deterioration of its insulating properties.

At this point, one can note that the dielectric constant and the leakage current of titanium silicates films vary in opposite ways with the increase of TiO_2 content (see Figs. 5 and 6). As a consequence, a trade-off should be made between a high- k value and a low leakage current. Thus, $x \sim 0.45$ arises as the composition that yields $\text{Ti}_x\text{Si}_{1-x}\text{O}_2$ films exhibiting an excellent combination of electrical properties [i.e., $k \sim 18$, $\tan(\delta) \sim 0.01$, and leakage current density of $5 \times 10^{-7} \text{ A/cm}^2$ at 1 MV/cm]. Finally, once the film composition is optimized, one may wonder to improve further the electrical properties of the $\text{Ti}_{0.5}\text{Si}_{0.5}\text{O}_2$ films by either depositing them at higher temperature or subjecting them to an appropriate postdeposition annealing treatment. The optimal thermal treatment should passivate the active defects (resulting from the room-temperature deposition) without initiating any phase precipitation in the films.

IV. CONCLUSION

Titanium silicate thin films have been successfully deposited from the concomitant sputtering of both SiO_2 and TiO_2 targets. The room-temperature deposition process developed here has enabled the deposition of dense and smooth $\text{Ti}_x\text{Si}_{1-x}\text{O}_2$ films over the entire composition range (i.e., from SiO_2 to TiO_2). The XPS and FTIR characterizations of the bonding states of the films have provided evidence that the titanium silicate films consist of a random mixture of TiO_2 and SiO_2 without the presence of segregated TiO_2 and/or SiO_2 phases. Both the dielectric and optical properties of the $\text{Ti}_x\text{Si}_{1-x}\text{O}_2$ films are shown to be highly sensitive to their composition. Indeed, we found that the films from the $\text{Ti}_x\text{Si}_{1-x}\text{O}_2$ system not only show good dielectric properties [$\tan(\delta) < 0.02$ and a very low dispersion] but also offer the latitude to control the dielectric constant from 4 up to 45 depending on their TiO_2 content. On the other hand, the optical band gap is found to decrease markedly as the TiO_2 content of the silicate films is increased. This variation is found to correlate well with the observed increase of the leakage current for TiO_2 -rich films. Finally, by achieving a

systematic investigation of the $\text{Ti}_x\text{Si}_{1-x}\text{O}_2$ films over the entire composition range, we were able not only to better understand the effect of Ti local environments on their polarizability but also to pinpoint the film composition that exhibits the best trade-off between high- k value and low leakage current density.

ACKNOWLEDGMENTS

This work was financially supported by MICRONET (the Network of Centers of Excellence on Microelectronic Devices, Circuits and Systems for ULSI), the Natural Science and Engineering Research Council (NSERC) of Canada, and DALSA Semiconductor.

- ¹*The International Technology Roadmap for Semiconductors 2003 Edition* (Semiconductor, Industry Association, Austin, TX, 2003).
- ²G. D. Wilk, R. M. Wallace, and J. M. Anthony, *J. Appl. Phys.* **89**, 5243 (2001).
- ³C. Durand, C. Dubourdieu, C. Vallée, V. Loup, M. Bonvalot, O. Joubert, and H. Roussel, *J. Vac. Sci. Technol. A* **22**, 655 (2004).
- ⁴S. J. Kim, B. J. Cho, M. F. Li, X. Yu, C. Zhu, A. Chin, and D.-L. Kwong, *IEEE Electron Device Lett.* **24**, 387 (2003).
- ⁵M. Kadoshima, M. Hiratani, Y. Shimamoto, K. Torii, H. Miki, S. Kimura, and T. Nabatame, *Thin Solid Films* **424**, 224 (2003).
- ⁶S.-Y. Lee, H. Kim, P. C. McIntyre, K. C. Saraswat, and J.-S. Byun, *Appl. Phys. Lett.* **82**, 2874 (2003).
- ⁷F. Mondon and S. Blonkowski, *Microelectron. Reliab.* **43**, 1259 (2003).
- ⁸D. Brassard, D. K. Sarkar, L. Ouellet, and M. A. El Khakani, *J. Vac. Sci. Technol. A* **22**, 851 (2004).
- ⁹D. Brassard and M. A. El Khakani, *J. Appl. Phys.* **98**, 054912 (2005).
- ¹⁰A. Paskaleva, A. J. Bauer, M. Lemberger, and S. Zürcher, *J. Appl. Phys.*

- 95**, 5583 (2004).
- ¹¹A. Nishiyama, A. Kaneko, M. Koyama, I. Fujiwara, M. Koike, M. Yoshiki, and M. Koike, in *Gate Stack and Silicide Issues in Silicon Processing II*, MRS Symposia Proceedings No. 670, edited by S. A. Campbell, C. C. Hobbs, L. Clevenger, and P. Griffin (Materials Research Society, Pittsburgh, 2001) Paper No. K4.8.1.
- ¹²D. K. Sarkar, E. Desbiens, and M. A. El Khakani, *Appl. Phys. Lett.* **80**, 294 (2002).
- ¹³G. D. Wilk, R. M. Wallace, and J. M. Anthony, *J. Appl. Phys.* **87**, 484 (2000).
- ¹⁴J. Price, P. Y. Hung, T. Rhoad, B. Foran, and A. C. Diebold, *Appl. Phys. Lett.* **85**, 1701 (2004).
- ¹⁵J. J. Chambers and G. N. Parsons, *J. Appl. Phys.* **90**, 918 (2001).
- ¹⁶A. Gibaud and S. Hazra, *Curr. Sci.* **78**, 1467 (2000).
- ¹⁷A. S. Ferlauto, G. M. Ferreira, J. M. Pearce, C. R. Wronski, R. W. Collins, X. Deng, and G. Ganguly, *J. Appl. Phys.* **92**, 2424 (2002).
- ¹⁸S. M. Rossnagel, *IBM J. Res. Dev.* **43**, 163 (1999).
- ¹⁹B. Gallas, A. Brunet-Bruneau, S. Fisson, G. Vuye, and J. Rivory, *J. Appl. Phys.* **92**, 1922 (2002).
- ²⁰X. Gao and I. E. Wachs, *Catal. Today* **51**, 233 (1999).
- ²¹G. B. Rayner Jr., D. Kang, and G. Lucovsky, *J. Vac. Sci. Technol. B* **21**, 1783 (2003).
- ²²S. Larouche, H. Szymanowski, J. E. Klember-Sapieha, L. Martinu, and S. C. Gujrathi, *J. Vac. Sci. Technol. A* **22**, 1200 (2004).
- ²³M. J. Alam and D. C. Cameron, *J. Sol-Gel Sci. Technol.* **25**, 137 (2002).
- ²⁴G. Ceriola, F. Iacona, F. La Via, V. Raineri, E. Bontempi, and L. E. Depero, *J. Electrochem. Soc.* **148**, F221 (2001).
- ²⁵X. Wang, H. Masumoto, Y. Someno, and T. Hirai, *Thin Solid Films* **338**, 105 (1999).
- ²⁶K. Guan, B. Lu, and Y. Yin, *Surf. Coat. Technol.* **173**, 219 (2003).
- ²⁷G.-M. Rignanese, X. Rocquefelte, X. Gonze, and A. Pasquarello, *Int. J. Quantum Chem.* **101**, 793 (2005).
- ²⁸S. van Huynenbroeck, S. Decoutere, R. Venegas, S. Jenei, and G. Winderickx, *IEEE Electron Device Lett.* **23**, 191 (2002).